Organic N and P in eutrophic fjord sediments - rates of mineralization and consequences for internal nutrient loading

Thomas Valdemarsen[1*], Cintia O. Quintana[1,2], Mogens R. Flindt[1] and Erik Kristensen[1]

[*]Corresponding Author: valdemarsen@biology.sdu.dk

[1)] Institute of Biology, University of Southern Denmark, Denmark

[2)] Instituto Oceanográfico, Universidade de São Paulo, São Paulo, Brazil

Key words: nutrient release, fluxes, reactivity, ammonium production, phosphate production, mineralization, oligotrophication, recovery, adsorbtion

Abstract

Nutrient release from the sediments in shallow eutrophic estuaries may counteract reductions of the external nutrient load and prevent or prolong ecosystem recovery. The magnitude and temporal dynamics of this potential source, termed internal nutrient loading, is poorly understood. We quantified the internal nutrient loading driven by microbial mineralization of accumulated organic N (ON) and P (OP) in sediments from a shallow eutrophic estuary (Odense Fjord, Denmark). Sediments were collected from 8 stations within the system and nutrient production and effluxes were measured over a period of ~2 years. DIN effluxes were high initially but quickly faded to low and stable levels after 50-200 d, whereas PO_4^{3-} effluxes were highly variable in the different sediments. Mineralization patterns suggested that internal N-loading would quickly (<200 days) fade to insignificant levels whereas internal PO_4^{3-} loading could be sustained for extended time (years). When results from all stations were combined, internal N-loading and P-loading from the fjord bottom was up to $121*10^3$ kg N yr^{-1} (20 kg N ha^{-1} yr^{-1}) and $22*10^3$ kg P yr^{-1} (3.6 kg P ha^{-1} yr^{-1}) corresponding to 6% (N) and 36% (P) of the external nutrient loading to the system. We conclude that the internal N-loading resulting from degradation of accumulated ON is low in shallow eutrophic estuaries, whereas microbial mineralization of accumulated OP is a potential source of P. Overall it appears that in N-limited eutrophic systems, internal nutrient resulting from mineralization of ON and OP in sediments is of minor importance.

1. Introduction

The nutrient loading of coastal ecosystems is often divided into internal and external sources, i.e. release from sediments resulting from organic N (ON) and P (OP) mineralization, and natural and anthropogenic supplies via the water shed and atmospheric deposition, respectively. The external nutrient loading can be quantified by summing up the external sources (e.g. Petersen et al. 2009). It is difficult, however, to use a mass balance approach to obtain reliable estimates of internal nutrient loading, since release from sediments and export to adjacent water bodies are difficult to quantify with sufficient temporal and spatial precision in large and dynamic estuaries with extensive spatial variability and open boundaries.

To complicate matters more, the internal nutrient loading can be divided into two fractions with different temporal dynamics. The first is rapid nutrient release from mineralization of fresh and newly deposited labile organic material, and the second is slow and continued nutrient release from mineralization of buried organic material with lower reactivity. High turnover of labile ON and OP deposited at the sediment-water interface ensures a rapid recycling of inorganic nutrients to the water column (Kelly & Nixon 1984; Valdemarsen et al. 2009). The primary productivity in many shallow estuaries is therefore partially controlled by nutrients released from the sediments (Cowan & Boynton 1996; Fullweiler et al. 2010; Mortazavi et al. 2012; Bukaveckas & Isenberg 2013). The contribution from mineralization of low reactivity and often deeply buried ON and OP to total sediment nutrient release, however, remains largely unknown. Nutrient release reported in most published studies is dominated by the nutrients generated by labile ON and OP mineralization due to the short time-scale applied for measurements. It is nonetheless important to obtain reliable estimates of the nutrient generation and efflux resulting from mineralization of low reactivity ON and OP. In many instances the recovery of eutrophic ecosystems after reductions of the external nutrient loading does not occur or only occurs after considerable delay (Kronvang et al.

2005). This may be caused by substantial release of nutrients, which have accumulated to high concentrations over time in the sediments exposed to eutrophication (Pitkanen et al. 2001; Carstensen et al. 2006). Such delayed nutrient release is thought to counteract reductions in the external nutrient load and cause delayed recovery.

Determining the magnitude and temporal dynamics of the internal nutrient loading originating from ON and OP accumulated in sediments requires detailed biogeochemical studies. Organic matter degradation in sediments follow exponential decay kinetics (Westrich & Berner, 1984; Burdige 1991; Valdemarsen et al. 2014) and inorganic nutrient production from ON and OP is therefore expected to decrease exponentially with time. Not all produced inorganic nutrients will result in internal nutrient loading, however, since chemical and biological processes within sediments lead to nutrient retention or transformation before efflux to the overlying water. NH_4^+, for instance, can be adsorbed to the sediment matrix (Mackin and Aller 1984), assimilated by microbes or benthic microalgae or microbially transformed to other nitrogeneous compounds (Christensen et al. 2000; Tyler & McGlathery 2003; Hulth et al. 2005). Coupled nitrification-denitrification in the oxic-anoxic transition of surface sediments, whereby NH_4^+ is converted to inert N_2-gas, is for instance an ecologically important process which reduces the amount of bioavailable N (Seitzinger 1988; Burgin & Hamilton 2007). Due to adsorbtion and denitrification, the efflux of dissolved inorganic nitrogen (DIN = $NH_4^+ + NO_3^- + NO_2^-$) is generally much lower than anticipated from total ON mineralization in the sediment (Mackin and Swider 1989). As for NH_4^+, PO_4^{3-} may adsorb to the sediment matrix; mainly to Fe-minerals in oxidized surface sediment (Sundby et al. 1992). PO_4^{3-} efflux is therefore generally low in marine sediments lined with an oxic surface layer (Sundby et al. 1992; Jensen et al. 1995; Viktorsson et al. 2013).

In this study an experimental approach was used to determine the internal nutrient loading resulting from long-term mineralization of accumulated ON and OP in various sediment

types of a large shallow, eutrophic estuary (Odense Fjord, Denmark). The goals of the study were two-fold; (1) to quantify the magnitude and temporal dynamics of internal nutrient loading resulting from mineralization of ON and OP accumulated in sediments and (2) to evaluate the role of internal nutrient loading for the recovery of eutrophic ecosystems. Sediment cores were collected from various locations representing the dominating sediment types and environments in the estuary. These were maintained in experiments lasting ~2 years, during which the mineralization of ON and OP and resulting effluxes of inorganic nutrients were measured with high spatial and temporal resolution. By comparing total inorganic nutrient production to effluxes, the fate of inorganic nutrients was elucidated. The total internal nutrient loading of the entire system was estimated based on the measured nutrient effluxes and the areal distribution of dominating sediment types. Finally, the importance of internal nutrient loading in shallow eutrophic ecosystems is evaluated.

2. Materials and methods

2.1 Study area

Odense Fjord is a shallow eutrophic estuary located on the island of Fyn, Denmark. It is divided into a 16 km^2 shallow inner basin and a 45 km^2 deeper outer basin, with average depths of 0.8 and 2.7 m, respectively (Fig. 1). The fjord is connected to Kattegat through a narrow opening in the northeast. The main external nutrient source to Odense Fjord is Odense River, which has a catchment area of 1095 km^2, consisting mainly of farmland and urban areas (Petersen et al. 2009). Odense Fjord was critically eutrophic in the past due to high external nutrient loading exceeding $3000*10^3$ kg N y^{-1} and $300*10^3$ kg P y^{-1} before 1990 (Petersen et al. 2009). The massive nutrient loading caused extensive problems with high pelagic primary production, low water transparency, hypoxic events and blooms of opportunistic macroalgae. Implementation of several water action plans has reduced the external nutrient loading considerably to current levels of about $2000*10^3$ kg

104 N y^{-1} and $60*10^3$ kg P y^{-1}. This has improved the ecological quality of the system, since hypoxia is
105 now rare and levels of opportunistic macroalgae have decreased. Nonetheless, excessive nutrient
106 levels and high primary production are still a problem in Odense Fjord, which may be due to high
107 and sustaining internal nutrient loading.
108
109 *2.2 Sampling of sediment and water*
110 Intact sediment cores were collected on 8 stations from 4 habitat types in Odense Fjord during
111 October and November 2009 (Fig. 1). The stations were chosen to cover all major sediment types in
112 the fjord; 3 stations (St 1-3) represented shallow silty sediments in the inner fjord, St 4 and 5
113 represented shallow (< 1 m) silty and sandy sediments in the outer fjord, respectively, and finally, 3
114 stations (St 6-8) represented deep (2-6 m) silty sediments in the outer fjord. A detailed survey of
115 sediment characteristics conducted in 2009 (partially presented in Valdemarsen et al. 2014)
116 revealed that the four selected habitat types (shallow silty inner fjord, shallow silty outer fjord,
117 shallow sandy outer fjord and deep silty outer fjord) represented 21, 11, 29 and 39% of the fjord
118 area, respectively. Fifteen sediment cores were sampled from each station with 30 cm long, 8 cm
119 internal diameter Plexiglas core liners. The shallow stations (St 1-5) were sampled from a dinghy
120 using a hand operated coring device. Cores from the deeper stations (St 6-8) were subsampled from
121 a 'HAPS' box corer on board a larger vessel ("Liv II", Danish Nature Agency). Water temperatures
122 were 10-12˚C at the time of sampling.
123 Seawater used for the experiment was collected at Kerteminde Harbor at various times
124 during 2009-2011. The seawater was GF/C-filtered and adjusted to the appropriate salinity (10 or
125 20) before it was used for experiments.

126 *2.3 Experimental setup*

Sediment cores were pre-treated before the experiment to assure that they had equal sediment height and were free of macrofauna. The sediment cores were adjusted to 20 cm depth by removing the bottom stopper and carefully removing excess sediment from below. After reinserting the bottom stopper, the overlying water was purged with N_2 for 30 min to induce anoxia and the top stopper was reinserted. Asphyxiated macrofauna was removed from the sediment surface after ~48 h in darkness.

The pre-treatment was completed 2-4 days after sampling and sediment cores were then transferred to the experimental setup consisting of eight ~70 L water tanks located in a temperature controlled room at 15˚C. The incubation temperature of 15˚C approximately corresponds to the average annual water temperature in Odense Fjord. Each tank contained all sediment cores from one station, and was filled with filtered seawater with salinity 10 for St1-3 and salinity 20 for St 4-8, corresponding to the average salinity in the inner and outer basins of Odense Fjord (Fyns Amt, 2006). The water reservoir in each tank was vigorously mixed and aerated by air pumps, and kept at a level 0.5 cm above the upper rim of the open core liners to assure mixing of the headspace. The tanks were kept in darkness and about 1/3 of the water was renewed with fresh seawater every 2 weeks.

The sediment cores were maintained in this setup for the entire experiment, which lasted 589-635 days, depending on station. The time when cores were first transferred to the incubation tanks is referred to as t = 0. At selected times, 3 random sediment cores from each station were temporarily removed for flux measurements, and at other times 3 sediment cores were removed permanently for porewater and solid phase analysis as well as anoxic sediment incubations (see detailed sections below).

2.4 Flux measurements

151 The net exchange of nutrients (DIN and PO_4^{3-}) between sediment and water was determined in flux
152 experiments with 3 random sediment cores from each station. Flux experiments were conducted
153 weekly during the first 30 days, monthly until day 180 and every 2-3 months to the end. One day
154 prior to flux measurements, the inside headspace wall of the cores designated for flux
155 measurements were cleaned with a Q-tip to avoid biased flux measurements resulting from bacterial
156 biofilms on the inner surface of core liners (Valdemarsen and Kristensen 2005). These cores were
157 removed from the incubation tanks the next day, equipped with 4 cm long magnetic stirring bars a
158 few cm above the sediment surface and placed around a central magnet rotating at 60 rpm. Initial
159 water samples were taken from all cores, before they were closed with rubber stoppers. The cores
160 were incubated in darkness for 4 hours initially and up to 24 hours at the end of the experiment,
161 before the rubber stoppers were removed and final water samples were taken. Nutrient samples
162 were stored frozen (-20˚C) until analyzed for NH_4^+, NO_x^- (NO_3^- + NO_2^-) and PO_4^{3-} on a Lachat
163 Quickchem 8500 Flow injection Analyzer.
164
165 *2.5 Core sectioning*
166 Three sediment cores from each station were sectioned into 2 cm intervals to 16 cm depth at various
167 times (after 1 day and 1, 7-8, 16-17 and 20-21 months). Core sectioning and subsequent sediment
168 and porewater handling was done inside a N_2-filled glovebag. Individual sediment slices were
169 homogenized and porewater for nutrient analysis was obtained after centrifugation of sediment
170 subsamples in double centrifuge tubes (10 min, ~500 g) and GF/C-filtration. Samples for NH_4^+ and
171 PO_4^{3-} were stored frozen (-20˚C) until analysis as described above.
172 Sediment characteristics were determined on subsamples from every depth interval
173 during the core sectioning on day 1. Grain size composition, loss on ignition (LOI), total organic C
174 (TOC) content, density and porosity was determined as described in Valdemarsen et al. (2014).

175 Total N (TN) was measured by elemental analysis on dried sediment subsamples on a Carlo Erba
176 CHN EA1108 Elemental Analyzer. Total P (TP) was extracted by boiling combusted sediment
177 subsamples for 1 h in 1 M HCl. After centrifugation (10 min, 500 g) the supernatants were stored
178 until analyzed for PO_4^{3-} by colorimetric analysis (Koroleff 1983).
179 During initial and final core sectionings, reactive Fe was extracted from ~0.2 g
180 sediment subsamples with 0.5 M HCl. After 30 min extraction on a shaking table and centrifugation
181 (10 min, 500 g) the supernatants were stored in 4 mL plastic vials at room temperature until
182 analysis. Supernatants were analysed for reduced Fe (FeII) and total Fe by the ferrozine method
183 before and after reduction with hydroxylamine (Stookey 1970; Lovley and Phillips 1987). Oxidized
184 iron (FeIII) was determined as the difference between Total Fe and FeII.
185 Linear dimensionless NH_4^+ adsorbtion coefficients were determined during the initial
186 core sectioning on wet sediment subsamples from 0-2, 4-6 and 8-10 cm depth intervals in NH_4^+-
187 adsorbtion experiments as described in Holmboe and Kristensen (2002). Sediment subsamples were
188 incubated for 2 d in slurries with different NH_4^+-concentrations (0, 1, 2 and 3 mM) and 10 mg/L
189 allylthiourea to inhibit nitrification. After centrifugation (10 min, 500 g) the supernatant was
190 decanted and adsorbed NH_4^+ was extracted from the sediment pellet in 2 M KCl (Mackin and Aller,
191 1984). Supernatants from slurries and KCl-extractions was stored frozen (-20˚C) and analyzed for
192 NH_4^+ by the salicylate-hypochlorite method (Bower and Holm-Hansen 1980).
193
194 *2.6 Jar experiments*
195 Closed anoxic sediment incubations (‘jar experiments’) were performed with sediment from
196 different depths (0-2, 4-6 and 8-10 cm) right after core sectionings. Jar experiments measure the
197 total anaerobic mineralization rates of ON and OP from temporal accumulation of metabolic end-
198 products (NH_4^+ and PO_4^{3-}) in the porewater and yields solid results under a wide range of

environmental and experimental conditions (Kristensen and Hansen 1995; Kristensen et al. 2011; Valdemarsen et al. 2012; Quintana et al. 2013). Sediment from different depths was homogenized and fully packed into 6-8 glass scintillation vials ('jars'), leaving no headspace. The jars were closed with screw caps and buried in anoxic sediment at 15˚C. Two jars were sacrificed at 3-5 day intervals for porewater extraction by centrifugation. The jars were fitted with a perforated lid containing a GF/C-filter inside before centrifugation and were then centrifuged head-down in a centrifuge tube (10 min, ~500 g). Extracted porewater was stored frozen (-20˚C) and analyzed for NH_4^+ and PO_4^{3-} by colorimetric analysis as described above.

2.7 Calculations and statistics

Initial area specific pools of TN and TP were calculated by depth integration (0-20 cm) of TN and TP content in individual sediment layers. Differences in area specific pools of TN and TP between stations were detected by one-way ANOVA followed by Tuckey's post hoc test. Data were log-transformed before statistical analysis when assumptions of homoscedasticity were not met (only TN). Area specific pools of FeIII were calculated by depth integration at the beginning (initial) and end (final) and compared by pairwise t-tests.

NH_4^+ adsorption coefficients (K_{NH}) in individual sediment layers were determined based on NH_4^+-adsorbtion experiments. Extracted NH_4^+ (µmol g dw sediment) was plotted against NH_4^+-concentration (µmol cm^{-3}) and the linear slope, K´, was determined by least squares regression. K_{NH} could hereafter be determined from the relationship $K_{NH} = ((1-\phi)/\phi)*\rho_{ds}*K´$, where ϕ is sediment porosity and ρ_{ds} is dry sediment density (Holmboe and Kristensen 2002).

Rates of microbial ON and OP mineralization in discrete depth intervals (0-2, 4-6 and 8-10 cm) were obtained from jar experiments by fitting the time dependent linear concentration change of NH_4^+ and PO_4^{3-} by least-squares regression (Aller and Yingst 1980). When slopes were

223 significant ($p < 0.05$) the volume specific reaction rates (nmol cm^{-3} d^{-1}) in individual depth layers
224 were calculated from the slopes and corrected for sediment porosity and adsorbtion (Kristensen and
225 Hansen 1995). The mineralization rates at 10-20 cm depth were calculated from exponential
226 regressions based on ON and OP mineralization rates in the top 10 cm. Total area specific ON and
227 OP mineralization were calculated by depth integration (0-20 cm) of measured NH_4^+ and PO_4^{3-}
228 production at different depths. The temporal patterns of total area specific ON and OP
229 mineralization were fitted to a double exponential decay regression model of the form $y = C_L*\exp(-$
230 $k_L*t) + C_R*\exp(-k_R*t)$, where t is time, C_L and C_R are constants and k_L and k_R denote the first order
231 decay constants for labile and refractory ON and OP, respectively. We hereby assume that
232 considerations based on organic C degradation kinetics (Westrich and Berner 1984) are also valid
233 for ON and OP mineralization. Half lives of labile and refractory ON and OP could hereafter be
234 calculated from the formula $T_{0.5} = \ln(2)/k´$, where $k´$ denote k_L and k_R.
235
236 **3. Results**
237 *3.1 Sediment characteristics*
238 Detailed sediment characteristics of the 8 stations in Odense Fjord were previously described in
239 Valdemarsen et al. (2014) and only a brief summary is given here. The sediments from all stations
240 had high sand content and variable silt-clay content with wet densities ranging from 1.2-1.8 g cm^{-3}
241 and porosities of 0.3-0.8. The medium grain size varied from 87 to 397 µm among stations. The
242 sediments from the innermost stations (St 1-3) and most of the stations in the outer basin (St 4 and
243 6-8) contained a high proportion of silt-clay particles (13-63%). Furthermore, the stations rich in
244 silt-clay particles were organic rich with 0.6-5.2% POC compared to the more sandy St 5 (0.1-0.2%
245 POC).

246 NH_4^+-adsorbtion coefficients varied erratically among stations and sediment depths
247 (Table 1). K_{NH} ranged from 0.14 in the 8-10 cm deep sediment on St 7 to 1.06 in the surface
248 sediment on St 2.
249 St 1 and St 3 from the inner basin had similar TN content ranging between 57-156
250 μmol cm^{-3} (Fig. 2). St 2 had slightly higher TN (103-227 μmol cm^{-3}) with a pronounced subsurface
251 peak occurring at 3 cm depth. In the outer basin the shallow and deep silty stations (St 4 and 6-8)
252 had similar TN-content (92-154 μmol cm^{-3}), except at the surface where TN was lower at St 4 (38-
253 60 μmol cm^{-3}). The sandy St 5 contained exceptionally low TN (8-16 μmol cm^{-3}). Depth integrated
254 TN was therefore lowest on St 5 (4.5 ± 0.1 mol N m^{-2}), intermediate at St 1 (13.5 ± 0.4 mol N m^{-2})
255 and similarly high on the remaining stations (16.0 to 21.4 mol N m^{-2}, Table 2).
256 Two of the stations in the inner basin (St 1 and 2) had similar TP profiles, with 10-11
257 μmol cm^{-3} at the sediment surface and a gradual decrease to 5.1-5.8 μmol cm^{-3} at 15 cm depth (Fig.
258 2). St 3 had the lowest TP content of the stations in the inner basin. The shallow silty sediments in
259 the outer basin (St 4) were similar to St 1-2 with respect to TP, whereas the shallow sandy sediment
260 (St 5) was similar to St 3. The deep silty sediments in the outer basin (St 6-8) were characterized by
261 constant TP with depth (9.6-13.5 μmol cm^{-3}). Depth integration showed that the highest area
262 specific TP content was found on the deep outer fjord stations (1.8-1.9 mol P m^{-2}), whereas shallow
263 silty sediments in the inner and outer fjord contained intermediate TP content (1.2-1.3 mol P m^{-2}; St
264 1, 2 and 4; Table 2). The lowest TP content (~0.7 mol P m^{-2}) was found on the silty St 3 and sandy
265 St 5 in inner and outer fjord, respectively.
266 Initial FeIII pools varied 30-fold between stations (6-243 mmol m^{-2}; Table 3), with the
267 lowest FeIII content found in shallow sandy sediment from the outer basin (St 5). FeIII only
268 constituted a minor fraction (2-10%) of total Fe on all stations. No statistically significant

differences were detected between initial and final FeIII-pools ($p > 0.17$), but there were trends towards higher final FeIII content, except on St 1 and 5.

3.2 ON and OP mineralization

Mineralization rates obtained in the fully anoxic jar experiments might have underestimated mineralization rates at the sediment surface, where O_2 can stimulate mineralization of O_2-sensitive organic matter (Hulthe et al. 1998). In coastal and estuarine sediments O_2 only penetrates to 1-3 mm depth, suggesting a minor importance of this artefact at the beginning of the experiment. Surprisingly the sediments did not become significantly more oxidized during the long term incubations as indicated by a modest build-up of oxidized FeIII and continuous presence of hydrogen sulfide in the porewater of surface sediment from all stations (data not shown). Hence we assume that mineralization rates in the sediment cores underlying an oxic water phase were closely approximated by the rates obtained in jar experiments.

NH_4^+ production in jar experiments was significant throughout the experiment, except for St 1, 8-10 cm depth after 607 d. Initially NH_4^+ production was highest in the surface 0-2 cm sediment from the silty St 1-2 in the inner fjord and the sandy St 5 in the outer fjord (159-338 nmol cm^{-3} d^{-1}) and was similar on remaining stations (63-101 nmol cm^{-3} d^{-1}; Fig. 3). Surface NH_4^+ production decreased rapidly over time in sediments from shallow locations in the inner and outer fjord, by 96% of initial rates on St 1 and by 61–82% on St 2–5. The surface NH_4^+ production in the sediments sampled in the deep outer basin (St 6–8) decreased by 8–67% during the experiment. NH_4^+ production at 4–6 cm depth was initially 18–60 nmol cm^{-3} d^{-1} on all stations and temporal changes were also observed in this layer, especially in shallow silty sediments from the inner basin where NH_4^+ production decreased by 75–96% to 1.4–12 nmol cm^{-3} d^{-1} by the end (Fig. 3). In sediments from the outer basin NH_4^+ production at 4-6 cm depth only decreased by 19-58%. At 8-

10 cm depth NH_4^+ production at all stations occurred at similar rates and showed similar temporal trends as observed at 4-6 cm depth (Fig. 3).

Significant PO_4^{3-} production was measured in the surface sediment from all stations throughout the experiment (Fig. 4). Initial rates were highest (30-35 nmol cm^{-3} d^{-1}) on St 1 and 2 from the shallow inner basin and considerably lower (7-18 nmol cm^{-3} d^{-1}) on the remaining stations. PO_4^{3-} production initially decreased rapidly in the surface sediment from St 1 and 2 and stabilized at relatively low and stable levels after ~200 d (0.7-6.0 nmol cm^{-3} d^{-1}). Surface PO_4^{3-} production also decreased over time on the other stations, but temporal trends were more erratic. PO_4^{3-} production in deeper sediment was generally lower than at the surface, and with less variability among stations (Fig. 4). PO_4^{3-} production at 4-6 cm depth was 0-6 nmol cm^{-3} d^{-1} and remained quite stable throughout the experiment on all stations. The only significant decrease ($p = 0.01-0.03$) occurred in silty sediments from the inner basin (St 1-3) and St 6 and 8 from the deep outer basin. PO_4^{3-} production varied between 0-5 nmol cm^{-3} d^{-1} at 8-10 cm depth and was stable throughout the experiment.

Area-specific ON mineralization was calculated by depth integration of NH_4^+ production rates (Fig. 3). The sediments from the inner basin (St 1-3) showed high initial ON mineralization (6-11 mmol m^{-2} d^{-1}) in the same range as the shallow silty and sandy sediments from the outer basin (6 and 10 mmol m^{-2} d^{-1} on St 4 and 5, respectively). The deep silty sediments from the outer basin showed the lowest initial ON mineralization (St 6-8; 3-5 mmol m^{-2} d^{-1}). Area specific ON mineralization decreased during the experiment on all stations, by 82-93% for the silty inner fjord and 34-71% on remaining stations. The temporal decrease was mainly driven by successively lower ON mineralization in surface sediment during the first ~200 d and area-specific ON mineralization was fairly constant hereafter. Initial area-specific OP mineralization was 0.2-1.0 mmol m^{-2} d^{-1} (Fig. 4) and decreased (59-70%) over time on several of the stations (St 1-3 and St 6).

As for ON mineralization, the successively lower OP mineralization was mainly due to decreased OP mineralization in surface sediment. On the other stations area-specific OP mineralization remained relatively high and did not show clear temporal trends.

Double exponential decay models fitted the ON mineralization kinetics on St 1-6 and the OP mineralization kinetics on St 1-3 and 6. Erratic mineralization patterns prevented the use of exponential decay models on remaining stations (see Fig. 3-4). Decay constants for labile and refractory ON and OP in were fairly similar at all stations, with k_L´s of 0.02-0.06 d^{-1} (except for 10 times higher values for ON at St 6 and for OP at St 2) and k_R´s of 0.0003-0.0015 (Table 4). The half lives for ON and OP were in the range of 0.01-0.11 and 1.3-6.3 years for labile and refractory fractions, respectively.

3.3 DIN- and DIP-fluxes

DIN fluxes followed a similar exponentially decreasing pattern for all stations (Fig. 5), and ranged from 1.1-3.7 mmol m^{-2} d^{-1} initially (t =0-90 d) to 0.09-0.5 mmol m^{-2} d^{-1} by the end. The main form of DIN released initially was NH_4^+, which contributed 59-100% of DIN-release. Subsequently the NH_4^+ efflux decreased while NO_x^- switched from uptake to release and after 0.5-1 y to the end of the experiment, 68-100% of the DIN was released as NO_x^-.

The 8 stations showed different patterns of PO_4^{3-} fluxes. The stations from the shallow inner basin, St 1-3, showed exponentially decreasing PO_4^{3-} fluxes over time (initial fluxes of 0.1-0.2 mmol m^{-2} d^{-1} decreasing to 0.01-0.05 mmol m^{-2} d^{-1} by the end; Fig. 5). Initial (day 0-90) PO_4^{3-} fluxes on the shallow silty St 4 was around zero, but increased to 0.07-0.14 mmol m^{-2} d^{-1} during d 90-360 of the experiment. The highest PO_4^{3-} fluxes (0.07-0.21 mmol m^{-2} d^{-1}) were observed on the TP-poor sandy St 5, particularly towards the end of the experiment, while the TP-rich outer fjord

stations 6-8 had the lowest and most irregular PO_4^{3-} fluxes ranging from slightly negative to 0.1 mmol m^{-2} d^{-1}.

3.4 PO_4^{3-} and NH_4^+ in porewater

Porewater nutrient concentrations increased gradually at all depths during the experiment (data not shown). NH_4^+ and PO_4^{3-} only increased moderately in the upper 2 cm, but accumulated to high levels in the deeper diffusion limited sediment. Depth-averaged initial porewater NH_4^+ concentration varied between 171-407 μM on the stations. The sandy St 5 showed the highest NH_4^+ accumulation over time with a depth-average of 1473 μM in porewater by the end. On the remaining stations, NH_4^+ only accumulated to 259-587 μM. Depth-averaged PO_4^{3-} concentrations at the beginning varied between 17-71 μM depending on station. As for NH_4^+, the nutrient-poor sandy St 5 showed the highest PO_4^{3-} accumulation to 368 μM compared with 43-170 μM on the other stations.

3.5 N- and P-budgets

Area-specific nutrient mineralization obtained in jar-experiments was used to calculate total ON and OP mineralization during the experiment. ON mineralization was fairly constant for all stations except St 5 (1.4 to 1.9 mol m^{-2}) corresponding to 8-10% of initial TN (Table 5). St 5, on the other hand, had 3-fold higher ON mineralization that accounted for 80% of the initial ON. A 3-fold range among stations was also evident for OP mineralization, but with lowest rates of 0.12-0.l8 mol m^{-2} at St 1-4 and the highest rates of 0.22-0.33 mol m^{-2} at St 5-8 (8-48% of initial TP). Interestingly, there was no apparent relationship between sediment TN and TP content and mineralization activity as some of the highest N- and P-mineralization rates were observed on the organic-poor St 5 (Table 4). DIN-effluxes, porewater accumulation and adsorbtion only accounted for 18-32% of total ON

364 mineralization, indicating that most of the generated NH_4^+ was not accounted for by our
365 measurements. For P, the sum of PO_4^{3-} efflux and porewater accumulation only accounted for 10-
366 48% of total OP mineralization.
367
368 **4. Discussion**
369 *4.1 Sediment nutrient content*
370 TN and TP in sediments from Odense Fjord were in the same range or higher than reported for
371 other eutrophic systems (e.g. Boynton and Kemp 1985; Cowan & Boynton 1996; Lomstein et al.
372 1998; Coelho et al. 2004; Viktorsson et al. 2013) emphasizing the history of intense eutrophication
373 in Odense Fjord. TN and TP in the silty sediments of Odense Fjord (all stations except St 5) were
374 remarkably similar and only varied ~1.5 (TN) and ~3 (TP) times among stations. Despite these
375 overall similarities, the silty sediments from the shallow inner basin showed higher initial ON- and
376 OP-mineralization and nutrient effluxes than silty sediments from the outer fjord. This could be due
377 to higher availability of labile ON and OP in the sediments from the inner basin, reflecting the
378 nutrient rich conditions in the inner compared to the outer basin (Petersen et al.2009).
379 The sandy St 5 was markedly different from the other stations. It had the lowest total
380 nutrient content and yet exhibited some of the highest rates of ON and OP mineralization. The
381 frequent erosion by wind driven waves in this area (Valdemarsen et al. 2010) and deep (>20 cm)
382 reworking by lugworms (*Arenicola marina*) (Riisgaard & Banta 1998; Valdemarsen et al. 2011)
383 may remove fine particles and refractory organic matter from St 5 sediments (Wendelboe et al.
384 2012) and prevent organic matter accumulation, hence explaining the low organic content on this
385 station. On the other hand, intense growth and burial of microphytobenthos and other reactive
386 detritus by the strong physical disturbance and vertical mixing, can explain the unexpected high TN
387 and TP reactivity of St 5 sediment.

A rough areal estimate based on the measured TN and TP content on the examined stations (Table 2) suggest that $12.6*10^6$ kg N and $3.7*10^6$ kg P are stored in the upper 20 cm of Odense Fjord sediments, corresponding to ~6 (N) and ~62 (P) years of the current annual external nutrient loading to the system.

4.2 Organic N and P mineralization

Microbial mineralization of ON and OP in Odense Fjord sediments led to marked release of inorganic nutrients, especially in the initial phase of the experiment. Initially there were strong vertical gradients of ON and OP mineralization in silty and sandy sediments from shallow environments, indicating that newly deposited and relatively labile organic matter was being degraded near the sediment surface, with the depth gradient reflecting a gradual and time-dependent depletion of labile ON and OP (Westrich & Berner 1984; Mackin and Swider 1989; Valdemarsen et al. 2014). It was expected that ON and OP mineralization would decrease with time at all depths due to diminishing reactivity of the organic pools. However, significant temporal decreases were only observed in surface sediments from shallow locations, whereas mineralization rates were surprisingly stable in the underlying sediment and the entire sediment column in the deep outer fjord. Assuming that organic matter degradation follows an exponential decay pattern, the lack of a detectable attenuation in mineralization rates over a ~2 yr period indicates very low initial reactivity of ON and OP in the deeper layers (Westrich & Berner 1984). Nevertheless, since ON and OP of low reactivity was present at high concentrations, it remained a significant source for inorganic nutrients.

Total jar-based microbial ON and OP mineralization over the ~2 years experimental period (Table 5) only accounted for a minor fraction of initial TN and TP in sediments from Odense Fjord suggesting that the standing stock of organic N and P will be a source of nutrients for

412 extended time. Decay constants from the exponential decay model suggested that labile ON and OP
413 was rapidly degraded on all stations within 10-240 d, whereas depletion of more refractory ON and
414 OP will only occur on decadal time-scales (8-40 years), indicating that depletion of buried and
415 degradable ON and OP in eutrophic ecosystems will take considerable time.
416
417 *4.3 Fate of inorganic nutrients*
418 NH_4^+ and PO_4^{3-} produced by microbial mineralization accumulated in porewater of all sediments
419 within the first 1-6 months and only changed slightly hereafter. However, over the whole
420 experiment, porewater accumulation explained only a minor fraction of the jar-based total ON and
421 OP mineralization (0.8-8.1%). It was also investigated if NH_4^+ adsorbtion to mineral surfaces was
422 an important N sink. Despite the large spatial heterogeneity of NH_4^+ adsorbtion, this process never
423 accounted for more than 1% of the total produced NH_4^+ over the whole experiment and was
424 therefore not quantitatively important.
425 Nutrient release to the overlying water was the most important route for inorganic
426 nutrients produced by microbial mineralization. We could not account for all the produced
427 nutrients, since nutrient mineralization in jar experiments exceeded DIN and PO_4^{3-} effluxes by 70-
428 84% and 62-93%, respectively. The missing NH_4^+ may have been lost through coupled nitrification-
429 denitrification (e.g. Mackin and Swider 1989; Quintana et al. 2013). The conspicuous shift from
430 NH_4^+ to NO_3^- release indicated that nitrification was an active process in all sediment types, and
431 denitrifying bacteria probably proliferated in the NO_3^--rich surface sediment. In the present case,
432 coupled nitrification-denitrification rates of 1-2 mmol m^{-2} d^{-1} are required to account for the missing
433 NH_4^+, which is within the range reported in previous studies (e.g. Nielsen et al. 1995; Christensen et
434 al. 2000; Tobias et al. 2003). On the other hand, the missing PO_4^{3-} must have been retained within
435 the sediments. Several studies suggest almost complete PO_4^{3-} retention in marine sediments with an

oxic sediment surface (Rozan et al. 2002; Viktorsson et al. 2013) where PO_4^{3-} adsorbs to oxidized FeIII-minerals preventing PO_4^{3-} efflux (Sundby et al.1992). Experimental studies suggest that every FeIII molecule can retain more than 0.5 PO_4^{3-} molecules (Gunners & Blomqvist, 1997; Rozan et al. 2002). Hence the FeIII levels on all the silty stations were sufficient to retain the missing PO_4^{3-}, especially when considering that 0.5 M HCl extractions only extracts a fraction of the available FeIII. On the sandy St 5 the FeIII levels were too low to account for the missing PO_4^{3-}, indicating that there were other PO_4^{3-} sinks. PO_4^{3-} adsorbtion in the anoxic sediment (Krom & Berner, 1980) or precipitation of PO_4^{3-}-$CaCO_3$ complexes (Coelho et al. 2004) are possible sinks that were not quantified in this experiment.

4.4 Internal nutrient loading

We calculated the potential internal nutrient loading in Odense Fjord resulting from microbial mineralization of ON and OP for a 2 y period based on the measured nutrient effluxes. Average nutrient fluxes were calculated for each sediment type, i.e. shallow inner fjord (St 1-3), shallow silty outer fjord (St 4), sandy outer fjord (St 5) and deep outer fjord (St 6-8). The monthly time-weighted DIN and PO_4^{3-} fluxes and the total areal distribution of the different sediment types in Odense Fjord were then used to calculate the total internal nutrient loading (10^3 kg N and P mo^{-1}) for each sediment type and for the whole ecosystem. Evidently these calculations do not represent the *in situ* internal nutrient loading, since effects of the otherwise continuous deposition of organic matter were omitted by the experimental setup. It can also be debated if all the released nutrients can be considered internal nutrient loading, since the mineralization of recently deposited organic matter in surface sediments drove the majority of nutrient release during the first ~200 d. This nutrient release is largely determined by the ecosystem primary productivity extending only a few years back, and is therefore closely coupled to the recent levels of external nutrient loading. In any case the

460 calculations represent the nutrient release resulting from the mineralization of slowly reacting ON
461 and OP, which have accumulated in the sediments.

462 The calculations show the magnitude of nutrient release driven by microbial
463 mineralization of sediment-bound ON and OP in eutrophic ecosystems (Fig. 6). Total DIN release
464 from the whole fjord bottom is equivalent to $121*10^3$ kg N y^{-1} (~20 kg N ha^{-1} y^{-1}) the first year after
465 sedimentation of new organic matter has ceased, but only $38*10^3$ kg N y^{-1} (~6.2 kg N ha^{-1} y^{-1}) the
466 second year, since ON effluxes decreased exponentially on all stations . The shallow sandy
467 sediments in the outer fjord were most important for the total fjord-wide N-release (39%), whereas
468 the remaining 3 sediment types contributed equally (16-23%). The numbers for internal N-loading
469 are impressive at first, but only correspond to maximum 2-6% (N) of the current external N-loading
470 to Odense Fjord (about $2000*10^3$ kg N y^{-1}; Petersen et al. 2009). In the shallow N-limited Odense
471 Fjord the internal N-loading can therefore only have minor effects for overall ecosystem
472 productivity. In any case the external N-loading is far more important for the overall primary
473 productivity and ecological status.

474 The internal P-loading showed different temporal dynamics than internal N-loading.
475 Total P-release from the whole fjord bottom was stable over time at rates of $21\text{-}22*10^3$ kg P y^{-1}
476 (~3.4-3.6 kg P ha^{-1} y^{-1}; Fig. 6) while internal N-loading decreased exponentially. The stability was
477 driven by the increasing P release in shallow sandy outer fjord sediment and constant P release in
478 deep outer fjord sediment. As for N, the shallow sandy sediments in the outer fjord was most
479 important for total internal P-loading (57%) and the remaining 3 sediment types contributed equally
480 (14-15%). The internal P-loading corresponded to 35-36% (P) of the current external P-loading to
481 Odense Fjord ($60*10^3$ kg P y^{-1}; Petersen et al. 2009) and thus potentially constitutes a stable and
482 significant P-source in the system. However, since Odense Fjord and most other temperate coastal

ecosystems are mostly N-limited (Howarth et al. 2011) it is uncertain to which degree this excess P will affect ecosystem productivity.

4.5 Ecological implications

In many shallow eutrophic estuaries the external nutrient loading has been reduced to induce oligotrophication, but lower nutrient concentrations in the recipient estuary often occurs after considerable delay and rarely corresponds proportionally to the reductions (Kronvang et al. 2005; Carstensen 2006). This indicates that a transient phase occurs, where accumulated nutrients are being released from the soils and sediments in the water shed and receiving estuary, respectively, while the system equilibrates to a new level of external nutrient loading. Our study shows the magnitude and temporal dynamics of the internal nutrient loading that can be expected in shallow estuaries recovering from eutrophication. It appears that internal N-loading will be insignificant during recovery since it only corresponded to 2-6% of the external N-loading in our example and decreased rapidly. Internal N-loading will therefore only lead to marginally elevated N-availability and have minor effects on primary productivity and eutrophication status. The results are different with respect to PO_4^{3-}, since the internal P-loading was stable and corresponded to >1/3 of the external P-loading. Internal P-loading may therefore be a significant source of dissolved PO_4^{3-} for extended time in shallow eutrophic estuaries, and at a sufficiently high level to counteract reductions in the external P-loading. Most shallow estuaries are N-limited (Conley et al. 2000; Howarth & Marinho 2006; Howarth et al. 2011) so a high internal P-loading might only exacerbate N-limitation while having no further consequences for ecological quality. Decreasing internal N-loading and stable internal P-loading could also lead to increased dominance of cyanobacteria, which have low requirements for dissolved N. However, major shifts in phytoplankton communities would only occur in systems where decreased internal nutrient loading results in markedly lower

507 DIN-concentrations in the water phase, i.e. in systems where N-loading is low and internal nutrient
508 sources dominate.

509 The estimates of internal nutrient loading presented here provide an illustrative
510 example, but the exact values are only valid for the experimental conditions and must be
511 extrapolated with caution. Microbial reaction rates and DIN and PO_4^{3-} release from sediments are
512 strongly influenced by ambient conditions. For instance, sediment macrofauna may stimulate the
513 rates of organic matter degradation and sediment nutrient release through bioturbation (e.g.
514 Kristensen et al. 2012; 2014) leading to higher internal nutrient loading than estimated from
515 defaunated sediment cores in this experiment. Similarly microbial mineralization processes and
516 hence sediment DIN and PO_4^{3-} release are strongly temperature dependent (Westrich and Berner
517 1988; Sanz-Lazaro et al. 2011) and the magnitude of internal nutrient loading will therefore vary
518 seasonally compared to our estimates based on a constant temperature experiment. Finally, in our
519 experimental setup we also omitted hydrodynamics and porewater advection which are known to
520 stimulate nutrient cycling in shallow permeable sediments (Cook et al. 2007; Huettel et al. 2014).
521 This will especially affect the estimated nutrient release from the sandy sediments from this study.
522 Given the multitude of factors influencing nutrient mineralization rates, the actual magnitude of
523 internal nutrient loading and related consequences for primary productivity will therefore follow a
524 seasonal pattern driven by e.g. temperature, hydrodynamics and composition and activity of benthic
525 fauna. Other environmental variables such as hypoxia in the water column may also influence the
526 magnitude of internal nutrient loading, since it hampers PO_4^{3-} retention by Fe-oxides (Azzoni et al.
527 2005; Mort et al. 2010; Viktorsson et al. 2013) and limits coupled nitrification-denitrification while
528 stimulating dissimilatory nitrate reduction to NH_4^+ (Christensen et al. 2000; Jäntti & Hietanen
529 2012). Ecosystems suffering from hypoxia may therefore experience a much higher internal nutrient
530 loading than measured in this experiment. A comparison between total ON and OP mineralization

and effluxes from this experiment, suggests that nutrient effluxes could potentially increase 3-6 (DIN) and 2-10 (PO_4^{3-}) times if there are no mechanisms to transform or retain inorganic nutrients at the sediment surface.

4.6 Conclusions

In this study we investigated the mineralization of organic N and P buried in the sediments from a shallow eutrophic estuary and obtained estimates of the magnitude and temporal dynamics of internal nutrient loading. Total internal N-loading, which attenuated rapidly, corresponded to only a minor fraction of the external N-loading and was therefore not important for the ecological state in the studied ecosystem. Total internal P-loading showed no temporal attenuation and was quantitatively more important as it corresponded to >1/3 of the external P-loading. However, the studied ecosystem was N-limited, and it is therefore uncertain if high internal P-loading will result in negative ecological effects. This study indicates that internal nutrient loading, and especially internal N-loading, is a transient phenomena that can only temporarily influence the recovery trajectory of ecosystems recovering from eutrophication. In turn, internal nutrient loading driven by mineralization of organic N and P in sediments, cannot explain the lack of recovery in shallow estuaries where external nutrient loading has been reduced.

5. Acknowledgements

The authors thank the people who have helped with sampling, experimental work or analysis during this experiment (the crew aboard Liv II, Birthe Christensen, Rikke Orloff Holm, Maria Del Mar Sánchez Huertas and Maria Jensen). This project was funded by the Danish Strategic Science Foundation through grant 09-063190/DSF.

6. References

Aller RC, Yingst JY (1980) Relationships between microbial distributions and the anaerobic decomposition of organic-matter in surface sediments of Long-Island Sound, USA. Marine Biology 56:29-42

Azzoni R, Gianmarco G, Viaroli P (2005) Iron-sulphur-phosphorous interactions: implications for sediment buffering capacity in a mediterranean eutrophic lagoon. Hydrobiologia 550:131-148

Bower CE, Holm-Hansen T (1980) A salicylate-hypochlorite method for determining ammonia in seawater. Canadian Journal of Fisheries and Aquatic Sciences 37:794-798

Boynton WR, Kemp WM (1985) Nutrient regeneration and oxygen-consumption by sediments along an estuarine gradient. Marine Ecology Progress Series 23:45-55

Bukaveckas PA, Isenberg WN (2013) Loading, Transformation, and Retention of Nitrogen and Phosphorus in the Tidal Freshwater James River (Virginia). Estuaries and Coasts 36:1219-1236

Burdige DJ (1991) The kinetics of organic-matter mineralization in anoxic marine sediments Journal of Marine Research 49:727-761

Burgin AJ, Hamilton SK (2007) Have we overemphasized the role of denitrification in aquatic ecosystems? A review of nitrate removal pathways. Frontiers in Ecology and Environment 5:89-96

Carstensen J, Conley DJ, Andersen JH, Aertebjerg G (2006) Coastal eutrophication and trend reversal: A Danish case study. Limnology and Oceanography 51:398-408

Christensen PB, Rysgaard S, Sloth NP, Dalsgaard T, Schwærter S (2000) Sediment mineralization, nutrient fluxes, denitrification and dissimilatory nitrate reduction to ammonium in an estuarine fjord with sea cage trout farms. Aquatic Microbial Ecology 21:73-84

578 Coelho JP, Flindt MR, Jensen HS, Lillebo AI, Pardal MA (2004) Phosphorus speciation and
579 availability in intertidal sediments of a temperate estuary: relation to eutrophication and
580 annual P-fluxes. Estuarine Coastal and Shelf Science 61:583-590
581 Conley DJ, Markager S, Andersen J, Ellermann T, Svendsen LM (2002) Coastal eutrophication and
582 the Danish National Aquatic Monitoring and Assessment Program. Estuaries 25:848-861
583 Cook PLM, Wenzhofer F, Glud RN, Janssen F, Huettel M (2007) Benthic solute exchange and
584 carbon mineralization in two shallow subtidal sandy sediments: Effect of advective pore-
585 water exchange. Limnology and Oceanography 52:1943-1963
586 Cowan JLW, Boynton WR (1996) Sediment-water oxygen and nutrient exchanges along the
587 longitudinal axis of Chesapeake Bay: Seasonal patterns, controlling factors and ecological
588 significance. Estuaries 19:562-580
589 Fulweiler RW, Nixon SW, Buckley BA (2010) Spatial and Temporal Variability of Benthic Oxygen
590 Demand and Nutrient Regeneration in an Anthropogenically Impacted New England Estuary.
591 Estuaries and Coasts 33:1377-1390
592 Fyns Amt (2006) Miljøfarlige stoffer og ålegræs i Odense Fjord. Fyns Amt, Natur- og
593 Vandmiljøafdelingen, Odense
594 Gunnars A, Blomqvist S (1997) Phosphate exchange across the sediment-water interface when
595 shifting from anoxic to oxic conditions - an experimental comparison of freshwater and
596 brackish-marine systems. Biogeochemistry 37:203-226
597 Holmboe N, Kristensen E (2002) Ammonium adsorption in sediments of a tropical mangrove forest
598 (Thailand) and a temperate Wadden Sea area (Denmark). Wetlands Ecology and Management
599 10:453-460

600 Howarth RW, Marino R (2006) Nitrogen as the limiting nutrient for eutrophication in coastal
601 marine ecosystems: Evolving views over three decades. Limnology and Oceanography
602 51:364-376
603 Howarth R, Chan F, Conley DJ, Garnier J, Doney SC, Marino R, Billen G (2011) Coupled
604 biogeochemical cycles: eutrophication and hypoxia in temperate estuaries and coastal marine
605 ecosystems. Frontiers in Ecology and the Environment 9:18-26
606 Huettel M, Berg P, Kostka JE (2014) Benthic Exchange and Biogeochemical Cycling in Permeable
607 Sediments. Annual Review of Marine Science 6:23-51
608 Hulth S, Aller RC, Canfield DE, Dalsgaard T, Engström P, Gilbert F, Sundbäck K, Thamdrup B
609 (2005) Nitrogen removal in marine environments: recent findings and future research
610 challenges. Marine Chemistry 94:125-145
611 Hulthe G, Hulth S, Hall POJ (1998) Effect of oxygen on degradation rate of refractory and labile
612 organic matter in continental margin sediments. Geochimica et Cosmochimica Acta 62:1319-
613 1328
614 Jantti H, Hietanen S (2012) The Effects of Hypoxia on Sediment Nitrogen Cycling in the Baltic
615 Sea. Ambio 41:161-169
616 Jensen HS, Mortensen PB, Andersen FO, Rasmussen E, Jensen A (1995) Phosphorous cycling in a
617 coastal marine sediment, Aarhus Bay, Denmark. Limnology and Oceanography 40:908-917
618 Kelly JR, Nixon SW (1984) Experimental studies of the effect of organic deposition on the
619 metabolism of a coastal marine bottom community. Marine Ecology Progress Series 17:157-
620 169
621 Koroleff F (1983) Determination of phosphorus. In: Grashof K, Erhardt M, Kremling K (eds)
622 Method of seawater analysis. Verlag Chemie, Weinheim

623 Kristensen E, Hansen K (1995) Decay of plant detritus in organic-poor marine sediment: Production
624 rates and stoichiometry of dissolved C and N compounds. Journal of Marine Research
625 53:675-702
626 Kristensen E, Mangion P, Tang M, Flindt MR, Holmer M, Ulomi S (2011) Microbial carbon
627 oxidation rates and pathways in sediments of two Tanzanian mangrove forests.
628 Biogeochemistry 103:143-158
629 Kristensen E, Penha-Lopes G, Delefosse M, Valdemarsen T, Quintana C, Banta G (2012) What is
630 bioturbation? The need for a precise definition for fauna in aquatic sciences. Marine Ecology
631 Progress Series 446:285-302
632 Kristensen E, Delefosse M, Quintana CO, Flindt MR and Valdemarsen T (2014) Influence of
633 benthic macrofauna on ecosystem functioning in a shallow Danish estuary. Frontiers in
634 Marine Science 1, Article 41
635 Krom MD, Berner RA (1980) Adsorbtion of phosfate in anoxic marine sediments. Limnology and
636 Oceanography 25:797-806
637 Kronvang B, Jeppesen E, Conley DJ, Sondergaard M, Larsen SE, Ovesen NB, Carstensen J (2005)
638 Nutrient pressures and ecological responses to nutrient loading reductions in Danish streams,
639 lakes and coastal waters. Journal of Hydrology 304:274-288
640 Lomstein BA, Jensen AGU, Hansen JW, Andreasen JB, Hansen LS, Berntsen J, Kunzendorf H
641 (1998) Budgets of sediment nitrogen and carbon cycling in the shallow water of Knebel Vig,
642 Denmark. Aquatic Microbial Ecology 14:69-80
643 Lovley DR, Phillips EJP (1987) Rapid assay for microbially reducible ferric iron in aquatic
644 sediments. Applied and Environmental Microbiology 53:1536-1540
645 Mackin JE, Aller RC (1984) Ammonium adsorption in marine sediments. Limnology and
646 Oceanography 29:250-257

647 Mackin JE, Swider KT (1989) Organic matter decomposition pathways and oxygen consumption in
648 coastal marine sediments. Journal of Marine Research 47:681-716
649 Mort HP, Slomp CP, Gustafsson BG, Andersen TJ (2010) Phosphorus recycling and burial in Baltic
650 Sea sediments with contrasting redox conditions. Geochimica et Cosmochimica Acta
651 74:1350-1362
652 Mortazavi B, Riggs AA, Caffrey JM, Genet H, Phipps SW (2012) The Contribution of Benthic
653 Nutrient Regeneration to Primary Production in a Shallow Eutrophic Estuary, Weeks Bay,
654 Alabama. Estuaries and Coasts 35:862-877
655 Nielsen, K., P. L, Rasmussen, P. (1995) Estuarine nitrogen retention independently estimated by the
656 denitrification rate and mass balance methods: a study of Norsminde Fjord, Denmark. Marine
657 Ecology Progress Series 119:275-283
658 Petersen JD, Rask N, Madsen HB, Jorgensen OT, Petersen SE, Nielsen SVK, Pedersen CB, Jensen
659 MH (2009) Odense Pilot River Basin: implementation of the EU Water Framework Directive
660 in a shallow eutrophic estuary (Odense Fjord, Denmark) and its upstream catchment.
661 Hydrobiologia 629:71-89
662 Pitkanen H, Lehtoranta J, Raike A (2001) Internal nutrient fluxes counteract decreases in external
663 load: The case of the estuarial eastern Gulf of Finland, Baltic Sea. Ambio 30:195-201
664 Quintana C, Kristensen E, Valdemarsen T (2013) Impact of the invasive polychaete Marenzelleria
665 viridis on the biogeochemistry of sandy marine sediments. Biogeochemistry 115:95-109
666 Riisgard HU, Banta GT (1998) Irrigation and deposit feeding by the lugworm Arenicola marina,
667 characteristics and secondary effects on the environment. A review of current knowledge. Vie
668 Milieu 48:243-257
669 Rozan TF, Taillefert M, Trouwborst RE, Glazer BT, Ma SF, Herszage J, Valdes LM, Price KS,
670 Luther GW (2002) Iron-sulfur-phosphorus cycling in the sediments of a shallow coastal bay:

671 Implications for sediment nutrient release and benthic macroalgal blooms. Limnology and
672 Oceanography 47:1346-1354
673 Sanz-Lazaro C, Valdemarsen T, Marin A, Holmer M (2011) Effect of temperature on
674 biogeochemistry of marine organic-enriched systems: implications in a global warming
675 scenario. Ecological Applications 21:2664-2677
676 Seitzinger SP (1988) Denitrification in fresh-wat*er and co*astal marine ecosystems - ecological and
677 geochemical significance. Limnology and Oceanography 33:702-724
678 Stookey LL (1970) Ferrozine - a New Spectrophotometric Reagent for Iron. Analytical Chemistry
679 42:779-781
680 Sundby B, Gobeil C, Silverberg N, Mucci A (1992) The phosphorous cycle in coastal marine
681 sediments. Limnology and Oceanography 37:1129-1145
682 Tobias C, Giblin A, McClelland J, Tucker J, Peterson B (2003) Sediment DIN fluxes and
683 preferential recycling of benthic microalgal nitrogen in a shallow macrotidal estuary. Marine
684 Ecology Progress Series 257:25-36
685 Tyler AC, McGlathery KJ, Anderson IC (2003) Benthic algae control sediment-water column
686 fluxes of organic and inorganic nitrogen compounds in a temperate lagoon. Limnology and
687 Oceanography 48:2125-2137
688 Valdemarsen T, Kristensen E (2005) Diffusion scale dependent change in anaerobic carbon and
689 nitrogen mineralization: True effect or experimental artifact? Journal of Marine Research
690 63:645-669
691 Valdemarsen T, Kristensen E, Holmer M (2009) Metabolic threshold and sulfide-buffering in
692 diffusion controlled marine sediments impacted by continuous organic enrichment.
693 Biogeochemistry 95:335-353

694 Valdemarsen T, Canal-Verges P, Kristensen E, Holmer M, Kristiansen MD, Flindt MR (2010)
695 Vulnerability of Zostera marina seedlings to physical stress. Marine Ecology Progress Series
696 418:119-130
697 Valdemarsen T, Wendelboe K, Egelund JT, Kristensen E, Flindt MR (2011) Burial of seeds and
698 seedlings by the lugworm Arenicola marina hampers eelgrass (Zostera marina) recovery.
699 Journal of Experimental Marine Biology and Ecology 410:45-52
700 Valdemarsen T, Bannister RJ, Hansen PK, Holmer M, Ervik A (2012) Biogeochemical
701 malfunctioning in sediments beneath a deep-water fish farm. Environmental Pollution 170:15-
702 25
703 Valdemarsen T, Quintana CO, Kristensen E, Flindt MR (2014) Recovery of organic-enriched
704 sediments through microbial degradation - implications for eutrophic estuaries. Marine
705 Ecology Progress Series 503:41-58
706 Viktorsson L, Ekeroth N, Nilsson M, Kononets M, Hall POJ (2013) Phosphorus recycling in
707 sediments of the central Baltic Sea. Biogeosciences 10:3901-3916
708 Wendelboe K, Egelund JT, Flindt MR, Valdemarsen T (2013) Impact of lugworms (*Arenicola*
709 *marina*) on mobilization and transport of fine particles and organic matter in marine
710 sediments. Journal of Sea Research 76:31-38
711 Westrich JT, Berner RA (1984) The role of sedimentary organic matter in bacterial sulfate
712 reduction: The G-model tested. Limnology and Oceanography 29:236-249
713 Westrich JT, Berner RA (1988) The efftect of temperature on rates of sulfate reduction in marine
714 sediments. Geomicrobiology Journal 6:99-117

Tables

Table 1. Dimensionless linear NH_4^+ adsorbtion coefficients, K_{NH}, for different sediment depths at St 1-8.

	St 1	**St 2**	**St 3**	**St 4**	**St 5**	**St 6**	**St 7**	**St 8**
0-2 cm	0.26	1.06	0.33	0.46	0.64	0.31	0.57	0.48
6-8 cm	0.52	0.76	0.49	0.45	0.82	0.51	0.62	0.36
8-10 cm	0.40	0.82	0.20	0.79	0.55	0.66	0.14	0.45

719 Table 2. Depth integrated (0-16 cm) area specific TN and TP content ± SE (n=3) on St 1-8.

720 Superscript capital letters indicate the grouping of data obtained by ANOVA and subsequent post

721 hoc analysis. Average TN:TP ratios are also shown.

	TN	**TP**	**TN:TP**
	(mol m^{-2})	(mol m^{-2})	-
St 1	13.5 ± 0.4^{A}	1.34 ± 0.04^{A}	10.1
St 2	21.5 ± 0.5^{B}	1.31 ± 0.02^{A}	16.4
St 3	16.0 ± 0.2^{B}	0.70 ± 0.06^{B}	22.9
St 4	16.6 ± 1.1^{B}	1.18 ± 0.06^{A}	14.1
St 5	4.5 ± 0.1^{C}	0.73 ± 0.04^{B}	6.2
St 6	17.1 ± 0.1^{B}	1.94 ± 0.03^{C}	8.8
St 7	18.1 ± 0.0^{B}	1.86 ± 0.05^{C}	9.7
St 8	19.5 ± 0.2^{B}	1.83 ± 0.03^{C}	10.7

722

723

724 Table 3. Initial and final depth integrated pools (0-20 cm) of FeIII ± SE (n=3) on St 1-8. t-tests
725 showed no significant difference between initial and final FeIII pools on any station.

	Initial		**Final**	
	FeII	**FeIII**	**FeII**	**FeIII**
	(mmol m^{-2})	(mmol m^{-2})	(mmol m^{-2})	(mmol m^{-2})
St 1	2390 ± 34	243 ± 24	2294 ± 153	92 ± 22
St 2	2302 ± 160	157 ± 32	2399 ± 189	271 ± 161
St 3	1356 ± 155	62 ± 25	1358 ± 154	109 ± 40
St 4	1054 ± 86	28 ± 20	996 ± 23	97 ± 37
St 5	258 ± 2	6.3 ± 1.0	274 ± 39	6.4 ± 1.2
St 6	1887 ± 37	75 ± 12	1813 ± 43	141 ± 40
St 7	2464 ± 105	52 ± 2.0	2142 ± 60	137 ± 48
St 8	1697 ± 63	156 ± 8.0	1813 ± 43	210 ± 89

726

727

Table 4. Double exponential regression statistics for the temporal trends of total ON and OP degradation in jar experiments. Total organic N (ON) and P (OP) degradation were fitted to the exponential decay function $y = C_L*\exp(-k_{L*}x) + C_R*\exp(-k_R*x)$, where C_L and C_R denote constants and k_L and k_R denote decay constants for labile and refractory organic ON and OP, respectively. Statistics were not calculated for St 7-8 (ON) and for St 4-5 and 7-8 (OP), since the temporal degradation patterns did not fit the double exponential decay model. $T_{L, 0.5}$, L and $T_{R, 0.5}$, R denote the half life (y) of labile and refractory ON and OP, respectively.

ON

	k_L	k_R	C_L	C_R	$T_{L, 0.5}$	$T_{R, 0.5}$
St 1	$4.6*10^{-2}$	$1.1*10^{-3}$	7.7	2.4	0.04	1.73
St 2	$2.3*10^{-2}$	$1.0*10^{-3}$	3.1	2.9	0.08	1.90
St 3	$5.3*10^{-2}$	$1.1*10^{-3}$	8.6	2.8	0.04	1.73
St 4	$4.3*10^{-2}$	$0.4*10^{-3}$	4.0	1.8	0.04	4.75
St 5	$5.7*10^{-2}$	$0.6*10^{-3}$	2.7	7.2	0.03	3.17
St 6	$52.4*10^{-2}$	$0.3*10^{-3}$	3.2	2.9	0.01	6.33
St 7	-	-	-	-	-	-
St 8	-	-	-	-	-	-

OP

	k_L	k_R	C_L	C_R	$T_{L, 0.5}$	$T_{R, 0.5}$
St 1	$3.9*10^{-2}$	$0.4*10^{-3}$	0.6	0.3	0.05	4.75
St 2	$56.0*10^{-2}$	$1.5*10^{-3}$	1.1	0.3	0.01	1.27
St 3	$2.2*10^{-2}$	$1.3*10^{-3}$	0.1	0.3	0.08	1.46
St 4	-	-	-	-	-	-
St 5	-	-	-	-	-	-
St 6	$1.7*10^{-2}$	$0.9*10^{-3}$	0.4	0.5	0.11	2.11
St 7	-	-	-	-	-	-
St 8	-	-	-	-	-	-

Table 5. N and P budgets for the experiment. Initial TN and TP are the depth integrated values based on initial measurements. ON and OP degradation were calculated based on area specific rates obtained from jar experiments. Total NH_4^+-, NO_x^-- and PO_4^{3-}-effluxes were calculated by time integration of effluxes over the entire experimental period. NH_4^+- and PO_4^{3-}-accumulation in porewater (pw) was calculated from the difference between initial and final pw profiles. NH_4^+ adsorbtion was calculated from initial and final pw-inventories of NH_4^+ and the average NH_4^+-adsorbtion coefficient for each station. Values in parentheses marked with * or ** represent percentage relative to initial TN and TP or total N and P mineralization, respectively.

N-mineralization	**St 1**	**St 2**	**St 3**	**St 4**	**St 5**	**St 6**	**St 7**	**St 8**
Initial TN (mol m^{-2})	13.5	21.5	16.0	16.6	4.5	17.1	18.1	19.5
ON degradation, jars (mol m^{-2})*	1.38 (10.2)	1.62 (7.5)	1.56 (9.8)	1.44 (8.6)	3.62 (80.1)	1.77 (10.1)	1.61 (8.9)	1.86 (9.6)
NH_4^+ efflux (mol m^{-2})**	0.26 (19.1)	0.10 (6.2)	0.23 (14.6)	0.15 (10.7)	0.38 (10.6)	0.09 (5.1)	0.27 (16.6)	0.12 (6.2)
NO_x^- efflux (mol m^{-2})**	0.15 (11.2)	0.21 (13.0)	0.19 (12.1)	0.11 (7.3)	0.18 (5.0)	0.22 (12.9)	0.17 (10.8)	0.20 (10.9)
NH_4^+ accumulation, pw (mol m^{-2})**	0.02 (1.6)	0.01 (0.7)	0.00 (0.0)	0.08 (5.9)	0.06 (1.6)	0.03 (1.8)	0.01 (0.7)	0.02 (1.3)
NH_4^+ adsorbtion (mol m^{-2})**	0.01 (0.7)	0.01 (0.6)	0.00 (0.0)	0.01 (0.4)	0.04 (1.0)	0.02 (1.0)	0.00 (0.2)	0.01 (0.6)
P-mineralization	**St 1**	**St 2**	**St 3**	**St 4**	**St 5**	**St 6**	**St 7**	**St 8**
Initial TP (mol m^{-2})	1.34	1.31	0.70	1.18	0.73	1.94	1.86	1.83
OP degradation, jars (mol m^{-2})*	0.16 (12.6)	0.12 (7.9)	0.18 (19.6)	0.13 (11.2)	0.29 (47.7)	0.28 (14.5)	0.22 (11.5)	0.33 (17.4)
PO_4^{3-} efflux (mol m^{-2})**	0.02 (12.6)	0.04 (38.0)	0.02 (16.8)	0.02 (15.8)	0.10 (27.8)	0.02 (7.4)	0.03 (12.8)	0.02 (6.5)
PO_4^{3-} accumulation, pw (mol m^{-2})**	0.01 (4.8)	0.01 (9.6)	0.00 (1.6)	0.00 (0.8)	0.02 (5.1)	0.01 (3.0)	0.00 (1.7)	0.01 (3.1)

Figures

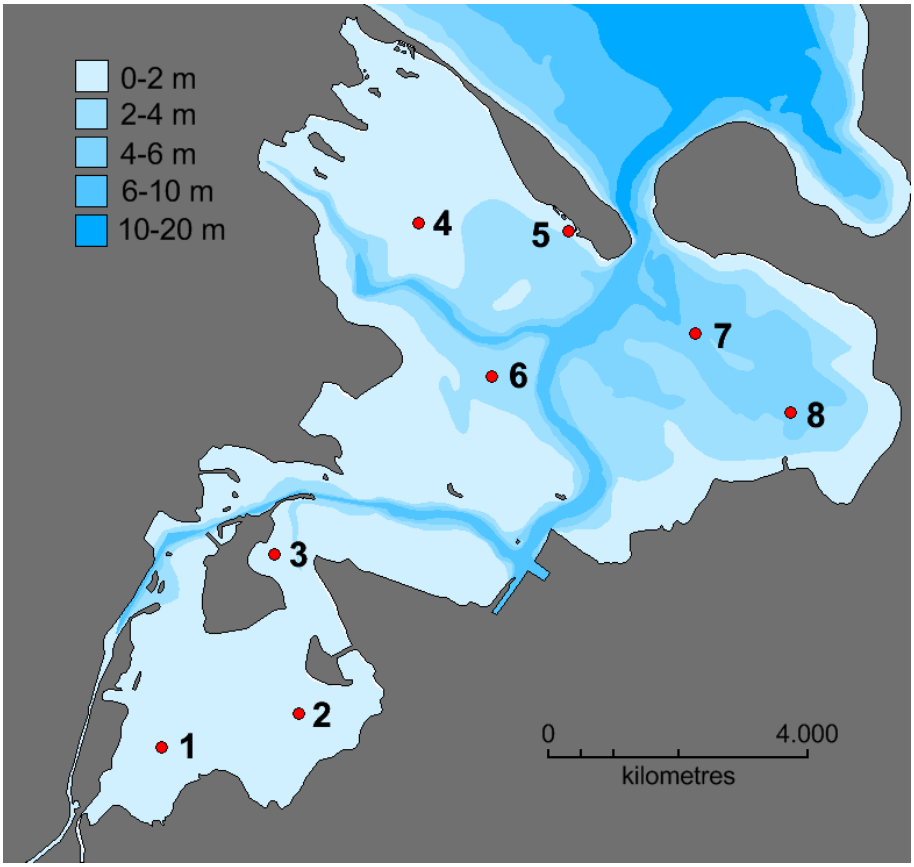

Figure 1. Map of Odense Fjord (55°29´15" N; 10°31´09") showing the 8 stations, where sediments were sampled for the long term degradation experiment. Gray color indicates land and different shades of blue indicate water depth.

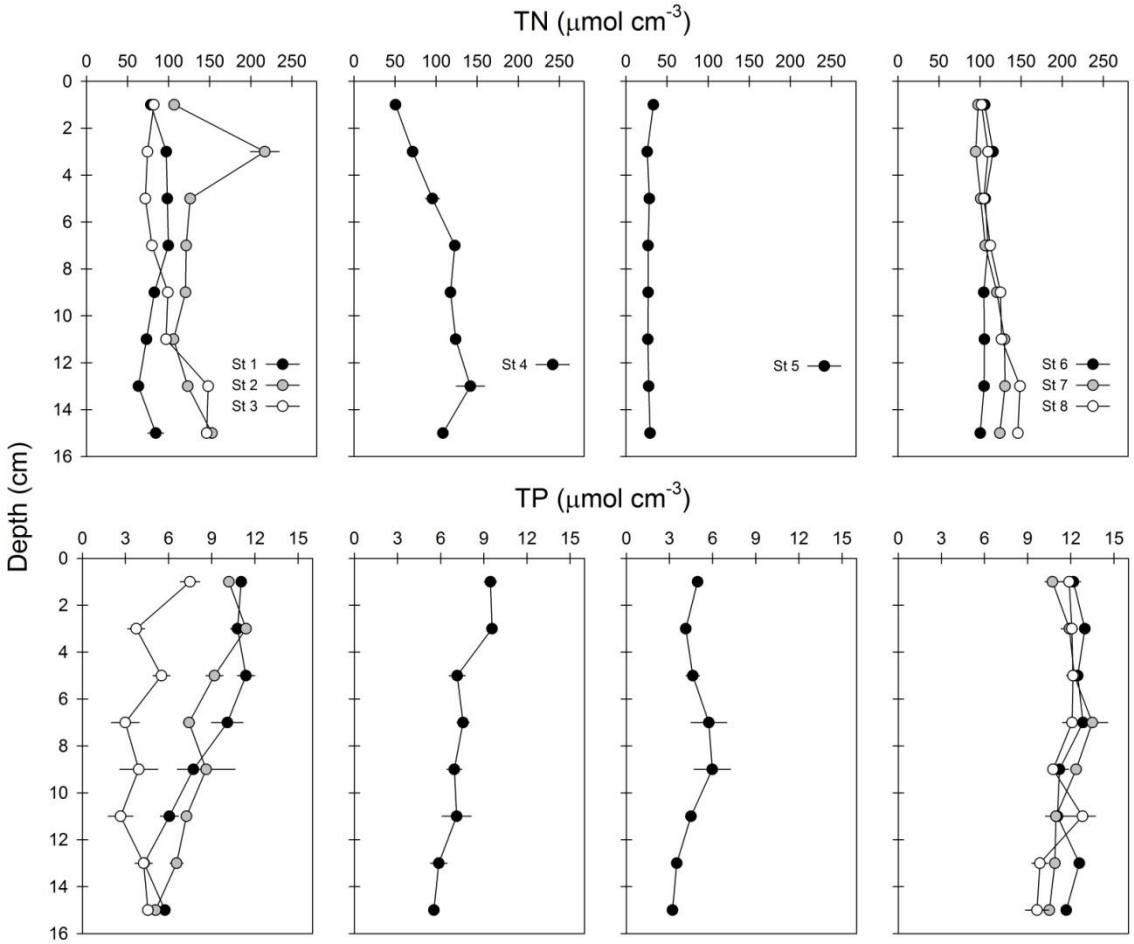

Figure 2. Total nitrogen (TN) and total phosphorus (TP) in sediments from Odense Fjord. Left panels show stations from the shallow inner fjord (St 1, 2 and 3), middle panels show shallow silty and sandy sediments in the outer fjord (St 4 and 5, respectively) and right panels show deep silty sediments in the outer fjord (St 6, 7 and 8). Error bars indicate standard error (n = 3).

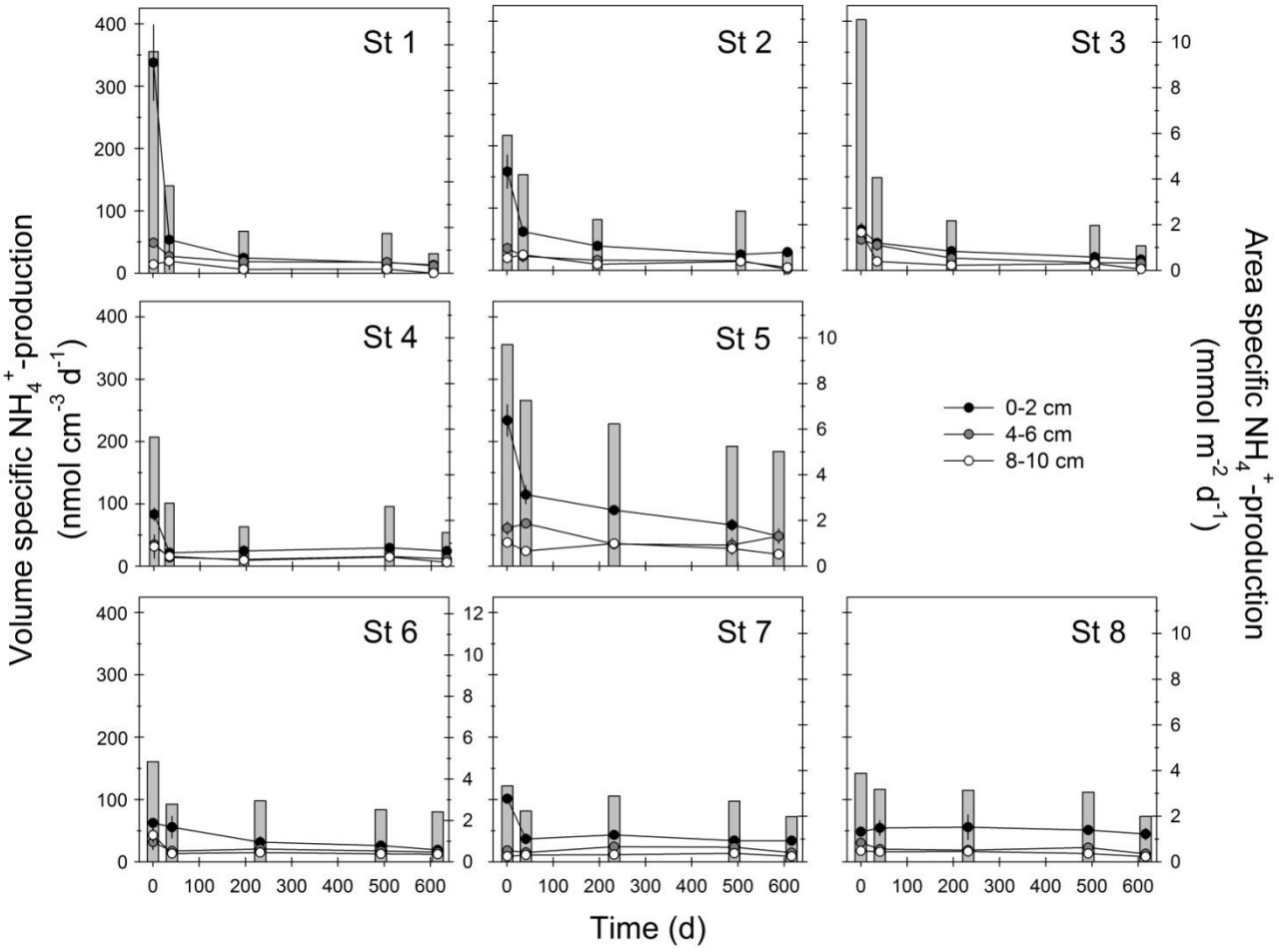

Figure 3. NH_4^+ production measured in jar experiments with sediment from shallow inner basin (upper panels), shallow silty and sandy outer basin (middle panels) and deep silty outer basin (lower panels). Black, gray and white symbols indicate volume specific NH_4^+ production in sediment from 0-2, 4-6 and 8-10 cm depth, respectively (left y-axis). Bars indicate depth integrated (0-20 cm) NH_4^+ production based on volume specific production rates (right y-axis).

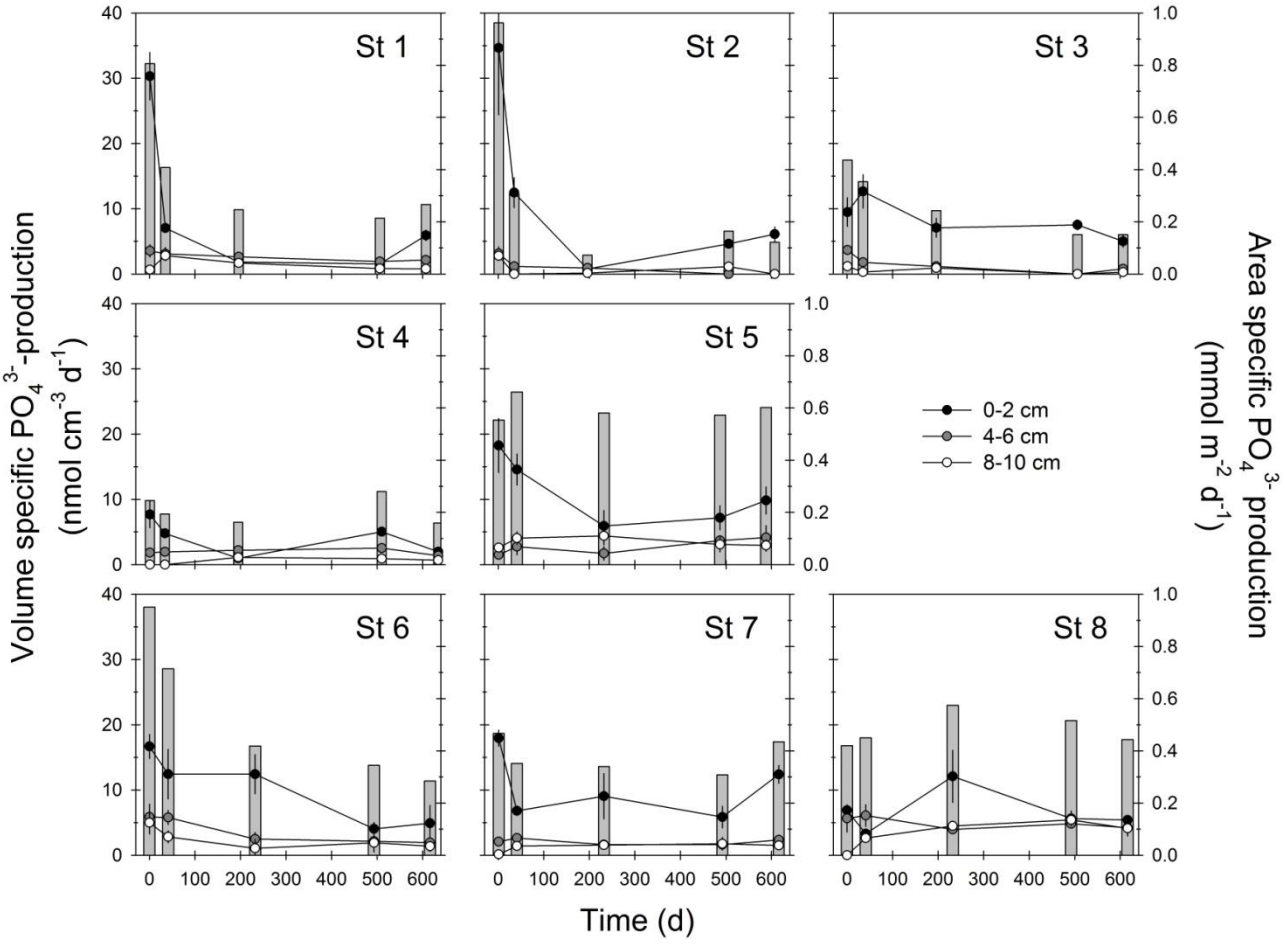

761

762 Figure 4. PO_4^{3-} production measured in jar experiments performed with sediment from shallow
763 inner fjord (upper panels), shallow silty and sandy outer fjord (middle panels) and deep silty outer
764 fjord (lower panels). Black, gray and white symbols indicate volume specific PO_4^{3-} production in
765 sediment from 0-2, 4-6 and 8-10 cm depth, respectively (left y-axis). Bars indicate depth integrated
766 (0-20 cm) PO_3^{3-} production based on volume specific production rates (right y-axis).

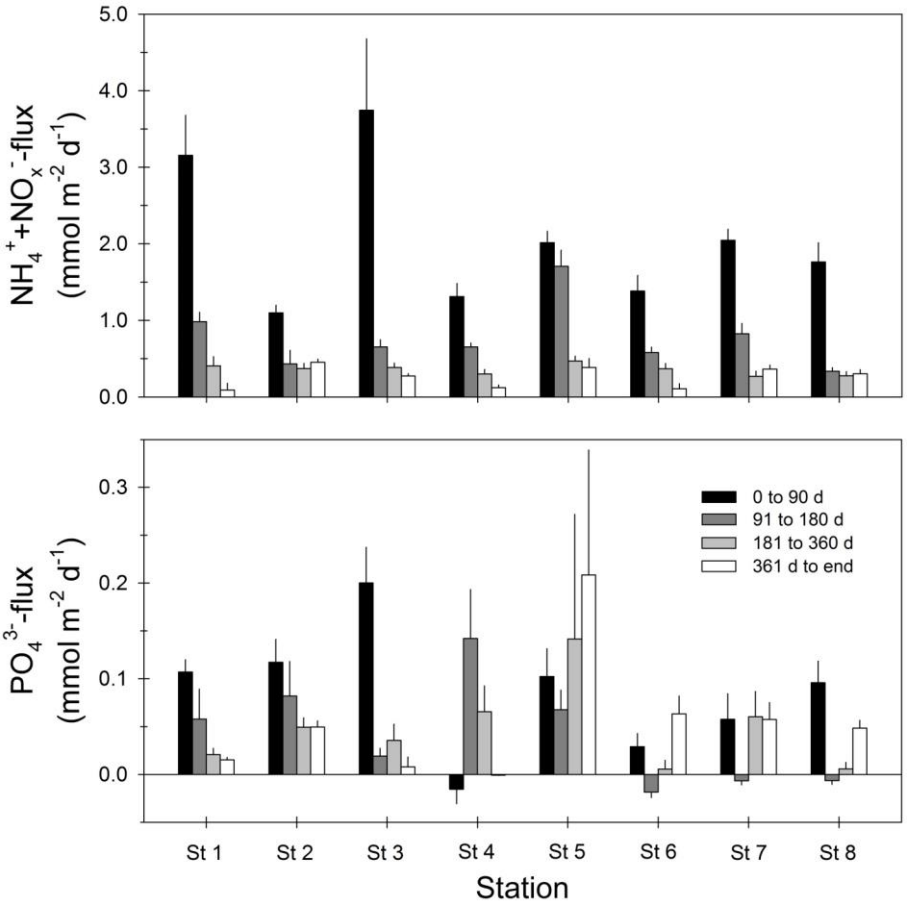

767

768 Figure 5. Fluxes of dissolved inorganic nitrogen (DIN = NH_4^+ + NO_X^-) and PO_4^{3-} at various times

769 during the experiment. Error bars represent standard error (n = 6-24).

770

771

772

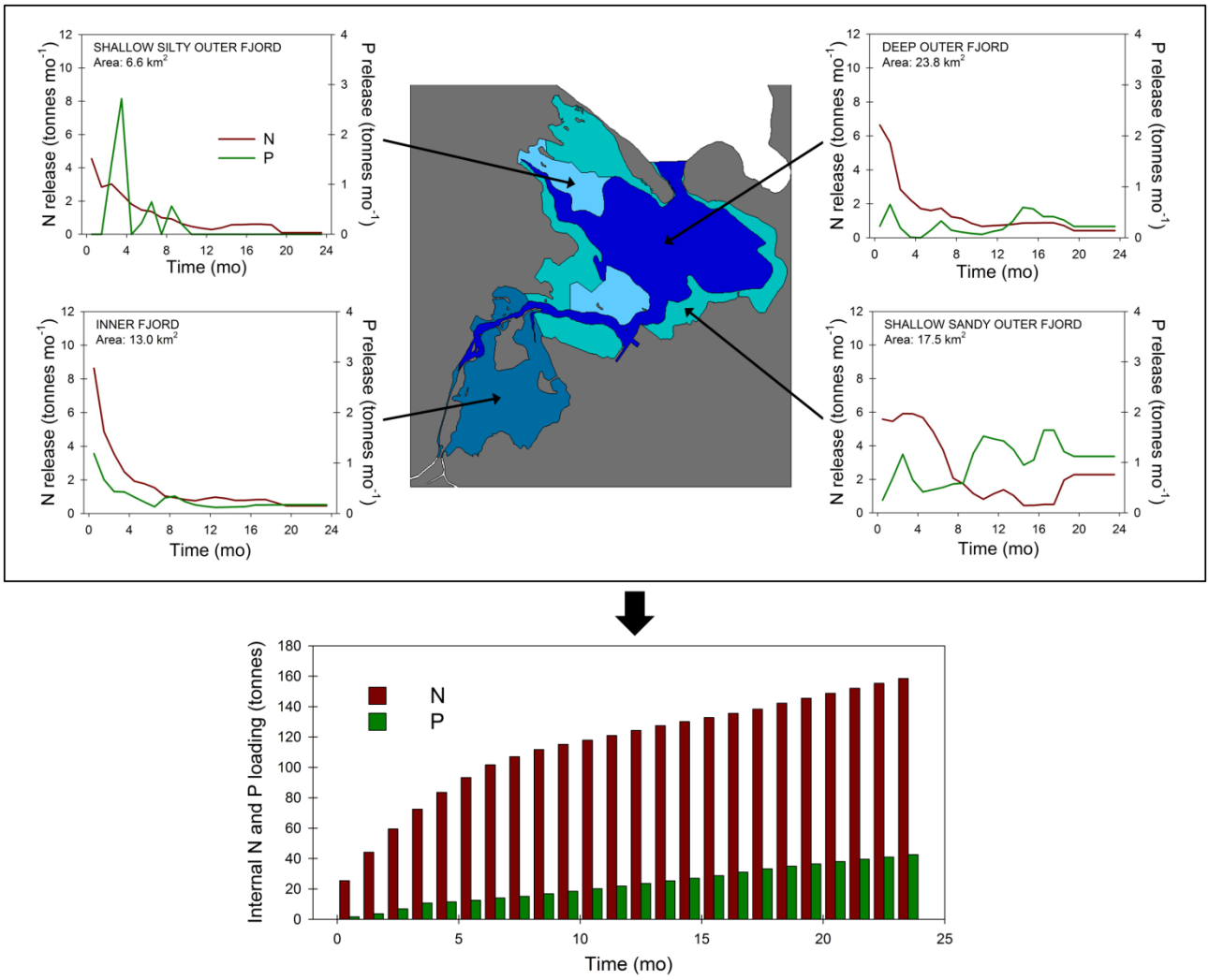

773

774 Figure 6. Estimated internal nutrient loading in Odense Fjord. The upper figure shows a schematic
775 overview of Odense Fjord with the distribution of sediment types included in this study and their
776 nutrient release over a 24 month period. The lower figure shows the cumulated nutrient release from
777 the entire fjord bottom.